Journal of Innovative Optical Health Sciences
Vol. 3, No. 3 (2010) 213–219

DOI: 10.1142/S1793545810001040

FUNDAMENTAL RESEARCH ON RADIOFREQUENCY ABLATION OF RAT BRAIN TISSUE BASED ON NEAR-INFRARED SPECTROSCOPY AND MIE THEORY

GUANGXIA HU*, ZHIYU QIAN*,‡, TIANMING YANG†,
WEITAO LI* and JIERU XIE*
*Department of Biomedical Engineering
Nanjing University of Aeronautics and Astronautics
29 Yudao Street, Nanjing 210016, China
†Zhongda Hospital, Southeast University
87 Dingjiaqiao Road, Nanjing 210009, China
‡zhiyu@nuaa.edu.cn

Near-infrared spectroscopy (NIRS) technology and Mie theory are utilized for fundamental research on radiofrequency ablation of biological tissue. Firstly, NIRS is utilized to monitor rats undergoing radiofrequency ablation surgery in real time so as to explore the relationship between reduced scattering coefficient (μ_s') and the degree of thermally induced tissue coagulation. Then, Mie theory is utilized to analyze the morphological structure change of biological tissue so as to explore the basic mechanism of the change of optical parameters caused by thermally induced tissue coagulation. Results show that there is a close relationship between μ_s' and the degree of thermally induced tissue coagulation; the degree of thermal coagulation can be obtained by the value of μ_s'; when biological tissue thermally coagulates, the average equivalent scattering particle decreases, the particle density increases, and the anisotropy factor decreases.

Keywords: Near-infrared spectroscopy (NIRS); Mie theory; radiofrequency ablation; reducing scattering coefficient (μ_s'); the average equivalent scattering particle radius.

1. Introduction

From the point of view of cell biology, biological tissue is composed of different sizes and different components of cells and interstitial cells. From the point of view of tissue optics, biological tissue is a typical optical turbid medium that includes light absorption and scattering simultaneously. Research indicates that there is an obvious change of optical properties, especially scattering properties, of biological tissue under thermal effect.[1,2] Radiofrequency ablation surgery, carried out on the target tissue by radiofrequency device to make the proteins coagulate, is a physical nerve block therapy. By quantitative analysis and research on the laws of optical transmission in biological tissue pre- and post-thermal coagulation, it is optical transmission in tissue is closely related to the optical parameters of biological tissue,[3–6] and found that the composition and structure of biological tissue change in thermal coagulation or lesions.[7–9] Obviously, the above knowledge has significant influence on the medical research and clinical applications of radiofrequency ablation and laser hyperthermia and on the development of medical equipments.[10]

‡Corresponding author.

In this paper, we studied the fundamental theory of radiofrequency ablation of biological tissue. Firstly, near infrared spectroscopy (NIRS) technology is utilized to explore the relationship between reducing scattering coefficient (μ_s') and the degree of thermally induced tissue coagulation. Then, from the morphological structure aspect, Mie theory is utilized to explore the basic mechanism of the change of optical parameters of biological tissue induced by heat coagulation.

2. Method

2.1. *Experimental system*

The experimental system (see Fig. 1) consists of two parts: the radiofrequency ablation system (8, 9) and the NIRS system (1–6). Both the radiofrequency temperature (38–100°C) and radiofrequency duration (0–100 s) can be adjusted using the radiofrequency ablation system. By using the NIRS system,[11] the spectral intensity of tissue can be measured in a minimally-invasive manner, in real time and *in vivo* in near-infrared region; real time display parameters of absorption coefficient (μ_a), reducing scattering coefficient (μ_s'), hemoglobin oxygen saturation (SO_2), oxy-hemoglobin concentration (C_{HbO_2}), deoxy-hemoglobin concentration (C_{Hb}), total hemoglobin concentration (C_{tHb}), cerebral blood flow (CBF) and cerebral blood volume (CBV) can also be calculated.

The optical parameter of μ_s' is analyzed in this paper. It is calculated by the following empirical Eq. (1).

$$\mu_s'(\lambda) = 3.1784 \cdot \exp(0.4314 \cdot S_{690-850}) \cdot \left(\frac{\lambda}{690}\right)^{(-0.1667 S_{690-850} - 0.4441)}. \quad (1)$$

Here $S690$–850 is the absolute value of the spectrum curve slope in the 690–850 nm wave band, λ is the wavelength. Equation (1) is obtained through intralipid and phantom model experiments and its accuracy is verified by OXImeter (96208, ISS Champaign, IL) using intralipid, phantom and rat models. Equation (1) is only applicable to the 100 μm probe and should be recalibrated for the other probes.[11]

2.2. *Radiofrequency ablation experiments*

Eighty normal rats (weight: 250 ± 20 g, 40 male, and 40 female) were selected and divided into eight groups randomly according to radiofrequency temperature: the control group (the not heated group), 42–45°C (the hypothermia group), 50°C, 55°C, 60°C, 65°C, 70°C and 75°C groups. Each group had 10 rats. The radiofrequency duration was 60 seconds.

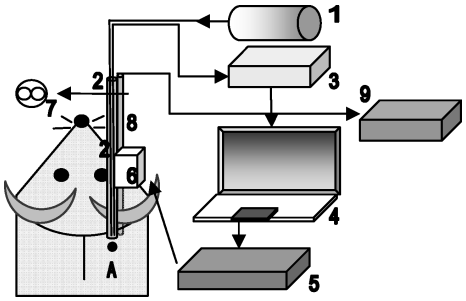

Fig. 1. Experimental system. (1) Halogen light source (HL-2000, Ocean Optics Inc. Dunedin, FL); (2) Y-shape fiber optic probe (diameter: 100 μm); (3) USB fiber optical spectrometer (USB2000, Ocean Optics Inc.); (4) Computer and software; (5) Stepper motor driver (MID-7604 National Instruments); (6) Stepper motor and controller (PCI-7344); (7) The section of fiber probe; (8) Radiofrequency electrode; (9) RF equipment (Leksell Neural RF instrument, Sweden Elekta).

First, radiofrequency electrode and NIRS probes were bound together in parallel, fixed in the stereotactic apparatus, and moved from the surgical hole to the target by the stepper motor. Then, the radiofrequency parameters were set and the radiofrequency ablation was started. After the ablation, radiofrequency electrode and NIRS probes were withdrawn with the stepper motor, the rat brain was removed, and pathological examination was immediately performed. During the course of radiofrequency ablation experiment, the optical parameters of target tissue were continuously recorded in real time including the pre- and post-states.

2.3. *Mie theory interpretation*

Mie scattering theory is an accurate mathematical solution of Maxwell's equations for parallel monochromatic light irradiation on an isotropic dielectric sphere in uniform medium using rigorous electromagnetic theory by G. Mie in 1908. Mie theory can be applied to study the scattering characteristics of biological tissue when the scattering effect of biological tissue is equivalent to that of spherical particles from a phenomenological point of view.[12,13] Supposing that there is irrelevant scattering between spherical particles, μ_s' can be expressed

by the following equation:

$$\mu_s'(\lambda) = \mathrm{N}_0 \sum_{i=1}^{p} f(r_i)(\pi r_i^2) Q_{\mathrm{scat}}(m, r_i, \lambda) \cdot [1 - g(m, r_i, \lambda)], \quad (2)$$

where r_i is the particle radius (for a specific biological tissue, its cellular and subcellular organs are non-single), $f(r_i)$ is the particle size distribution function, N_0 is the particle density, m is the relative refractive index of the scattering particles to the surrounding medium ($m = n_1/n_2$, n_1 and n_2 are the refractive index inside and outside the particles, respectively), and λ is the wavelength. $Q_{\mathrm{scat}}(m, r_i, \lambda)$ and $g(m, r_i, \lambda)$, calculated by Mie theory directly, are dimensionless scattering efficiency factor and anisotropy factor of single scattering particle, respectively.[14,15]

2.4. *Morphological study by use of Mie theory*

Firstly, μ_s' at the wavelengths of 690, 710, 730, 750, 770, 790, 810, 830, and 850 nm are induced by radiofrequency ablation experiment and are normalized at 770 nm so as to eliminate the influence of particle density. Then, comparing the nine normalized data sets with Mie theory results from Eq. (2) (also normalized at 770 nm) using the least square method, the average equivalent scattering particle radius can be effectively estimated $\left(r = \sum_i r_i f(r_i)\right)$. Lastly, with the average equivalent scattering particle radius established, the particle density can then be estimated by comparing the original nine data sets (no normalization) with Mie theory results reusing the least square method.[14–16]

3. Results and Analysis

3.1. *Results of radiofrequency ablation experiments*

Four types of μ_s' curves are found in the experiments (see Fig. 2, in which the gray column represents the radiofrequency period). Figure 2(a) represents the characteristic curve of μ_s' of one control group rat. It shows that μ_s' is relatively stable during the whole process. Figure 2(b) represents μ_s' of one hypothermia group rat (radiofrequency parameters: 44°C, 60 s). It shows that μ_s' increases gradually at the beginning of radiofrequency ablation, then gradually returns to the initial state after the end of radiofrequency ablation, and then becomes stable. All the μ_s' curves of the hypothermia group rats have the same trend. Figure 2(c) represents μ_s' of one heat group rat (radiofrequency parameters: 50°C, 60 s). It shows that μ_s' increases gradually at the beginning of radiofrequency ablation, then decreases slowly but still higher than the initial state after the end of radiofrequency ablation, and lastly becomes stable. All the μ_s' curves of the 50°C and 55°C groups of rats have the same trend. Figure 2(d) represents μ_s' of one "heat" group rat (radiofrequency parameters: 70°C, 60 s). It shows that μ_s' increases gradually at the beginning of radiofrequency ablation and then becomes stable after the end of radiofrequency ablation. All the μ_s' curves of the 60°C, 65°C, 70°C and 75°C groups of rats have the same trend. The statistical average of μ_s' is $16.91 \pm 1.71\,\mathrm{cm}^{-1}$ before thermal ablation and increases to $19.79 \pm 1.76\,\mathrm{cm}^{-1}$ after thermal ablation.

3.2. *Results of pathological examinations*

Results of pathological examinations are analyzed and summarized. For the control group rats, there is no necrosis and edema. For the hypothermia group rats, there is edema and a small amount of inflammatory cell infiltration in the damage zone, but no cell degeneration and necrosis. Most rats of 50°C and 55°C groups show a small area of damage foci and incomplete cell necrosis: usually, nerve cells degeneration and necrosis follow mixed distribution, or cells are piecemeal necrosis, accompanied by inflammatory cell infiltration and edema. All the rats of 60°C, 65°C, 70°C and 75°C groups show exact damage foci (see Fig. 3): the center of the damage foci is the necrosis zone showing complete nerve cell degeneration and necrosis (see Fig. 4); the edge of the necrosis zone is the narrow zone of cell degeneration and nuclear condensation; the adjacent to the narrow zone is the surrounding brain tissue edema zone showing a marked vasodilation and inflammatory cell infiltration (see Fig. 5); the outermost is the normal nerve cells.

3.3. *Results of Mie theory simulation*

Numerical method with MATLAB6.5 is applied in this paper.[16] Suppose that particle size distribution follows exponential function and covers the range from 1 nm to 1000 nm.[17] Given $f(r_i) = 1 \times 10^{10} \times \exp(-9.5 \times 10^{-4} r_i)$, the average equivalent

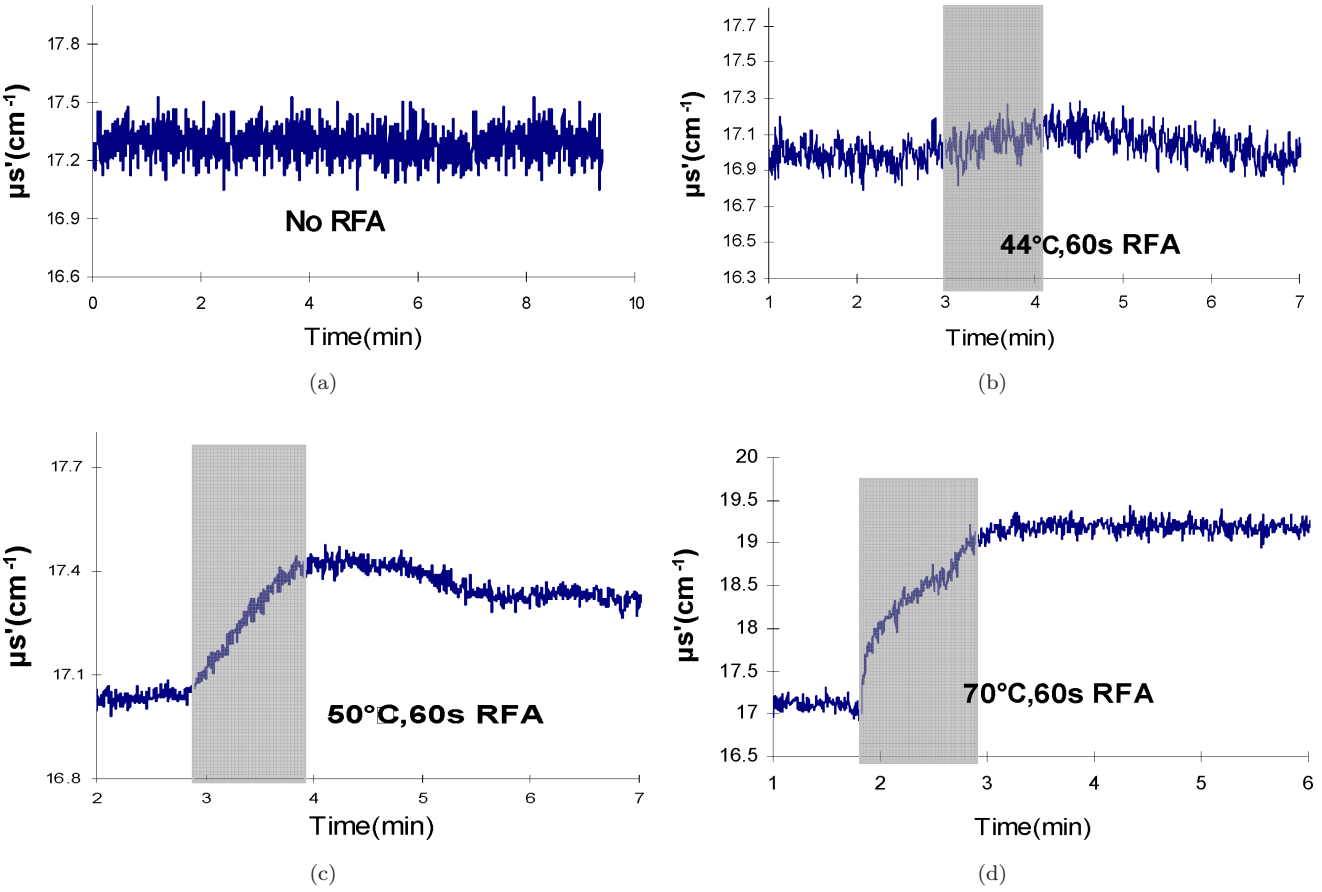

Fig. 2. Characteristic curves of μ_s' with different radiofrequency parameters. (a) The control group; (b) The hypothermia group; (c) The 50°C group; (d) The 70°C group.

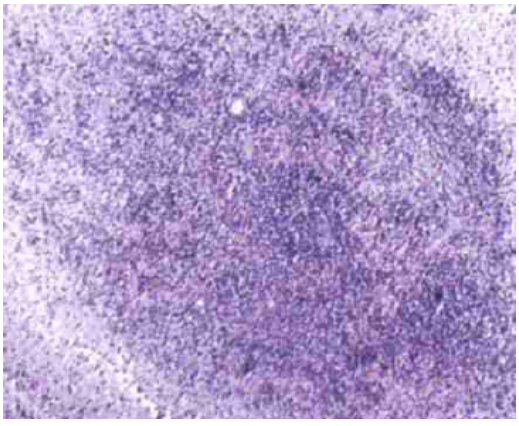

Fig. 3. The central necrosis cells and the surrounding edema (HE × 40).

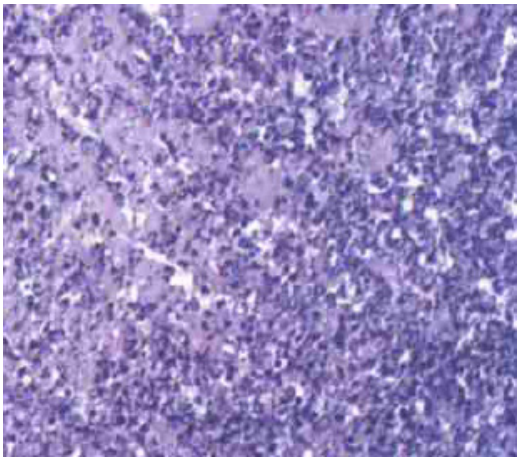

Fig. 4. The central necrosis cells (HE × 100).

scattering particle radius is determined. The comparison of μ_s' with three different sets of relative refractive index is shown in Fig. 6. The figure indicates that as the relative refractive index increases, the value of μ_s' increases. The values of μ_s' are normalized at 770 nm (inset graph in Fig. 6). It is clear that the shapes of normalized μ_s' with different relative refractive index are almost identical.

Given $m = 1.1$, simulation results of morphological change are shown in Table 1. When biological tissue thermally coagulates, its average

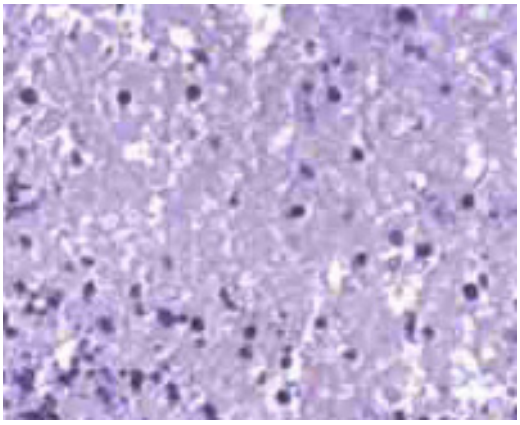

Fig. 5. The surrounding edema (HE × 100).

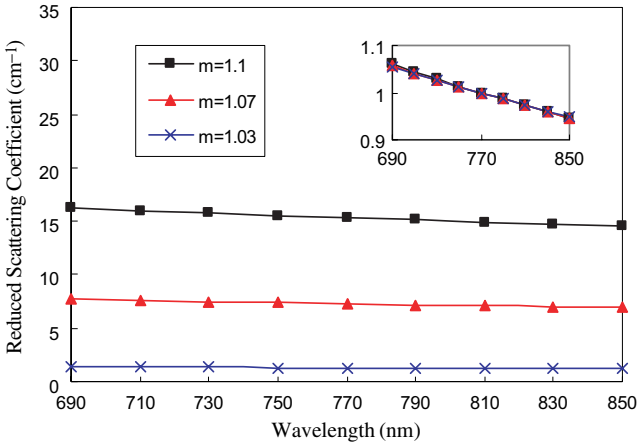

Fig. 6. Results of μ_s' with different relative refractive index.

Table 1. Results of Mie scattering simulation.

	μ_s' (cm^{-1})	r (nm)	N_0 ($\times 10^{17}\,m^{-3}$)	g
Before ablation	16.91	80	1.05	0.8015
After ablation	19.79	73	1.52	0.7778

equivalent scattering particle radius decreases from 80 nm to 73 nm, particle density increases from $1.05 \times 10^{17}\,m^{-3}$ to $1.52 \times 10^{17}\,m^{-3}$, and the anisotropy factor decreases from 0.8015 to 0.7718.

4. Discussions

For the hypothermia group (44°C) rats, results of radiofrequency ablation experiments show that μ_s' changes little, which increases at the beginning of heating and then decreases to the original level after the end of heating. Results of the pathological examination show that there is no thermal coagulation tissue. It indicates that, at this temperature, there is no denaturation of brain tissue proteins and no change of biological characteristics. For rats of 50°C and 55°C groups, results of radiofrequency ablation experiments show that μ_s' increases gradually at the beginning of heating, then declines a little after the end of heating, and lastly remains stable above the initial level. Results of the pathological examination show that there is solidification phenomenon for brain tissue close to the radiofrequency probe and both solidification and the surrounding edema are in the 1 mm zone just in front of the ablation probe. It indicates that both 50°C and 55°C have exceeded the critical temperature for protein denaturalization and so protein denaturation occurs in the brain tissue. But due to the low temperature or rather short radiofrequency time, there is less degree of denaturalization and smaller radius of lesion foci that cannot cover the effective detection area of the near-infrared probe.[18] Therefore there is a slight decline for μ_s' after the end of heating. For rats of 60°C, 65°C, 70°C and 75°C groups, results of radiofrequency ablation experiments show that μ_s' changes irreversibly and remains stable after the end of heating. Results of the pathological examination show that the damage foci cover almost all the effective detection area. It indicates that there is higher radiofrequency temperature and higher degree of protein denaturalization. Therefore μ_s' changes more significantly and remains stable after the end of heating. It can be concluded that there is a close relationship between μ_s' and the degree of thermal coagulation of biological tissue; the degree of thermally induced tissue coagulation can be obtained by the value of optical parameter μ_s'; it is around 50°C for the critical temperature of reversible and irreversible changes of biological tissue.

For the simulation model of Mie theory, the scattering between particles is assumed as irrelevant scattering. Theoretically, it can be regarded as irrelevant scattering approximately only when the scattering particles are single and the particle spacing is three times more than its diameter. Actually, tissue particles are quite compact, therefore it is not the absolute physical size, but an equivalent concept for the average equivalent scattering particle radius calculated by Mie theory. For the particle size distribution, Bartek *et al.*[17] reveals that it appears in exponential function for most cellular tissues. In this paper, $f(r_i) = A \times \exp(B \times r_i)$, where the

amplitude A does not influence the results, therefore it can be any reasonable value. The value of B can be changed to change the size distribution and the particle size.

Results, calculated with the same exponential size distribution and average particle size but with different relative refractive index of $m = 1.1$, 1.07, 1.03, show that normalized μ_s' values with different relative refractive indices are almost identical. In this paper normalized values are used to calculate the particle size. Therefore, the assumption in Eq. (2) that relative refractive index is the same for pre- and post-thermal coagulation appears reasonable. The value of relative refractive index does not influence the accuracy of the average particle size but the particle density. Results of average particle size have more reference value than the particle density.

Simulation results of morphological change show that, when biological tissue is heated to coagulation, the average equivalent scattering particle radius decreases from 80 nm to 73 nm and that the particle density increases from $1.05 \times 10^{17}\,\mathrm{m}^{-3}$ to $1.52 \times 10^{17}\,\mathrm{m}^{-3}$ and the anisotropy factor decreases from 0.8015 to 0.7718. For the average equivalent scattering particle radius, there is the same trend, but larger absolute value difference compared with the literature (values of Nilsson *et al.*[19] and Swartling *et al.*[20] decreased from 0.30 μm to 0.29 μm and from 0.29 μm to 0.25 μm, respectively). The trend can be analyzed in terms of histology. When biological tissue coagulates by heating, the organelles in cytoplasm disintegrate into pieces and granulars, the nucleus condenses, and vacuolation is generated. Therefore the average equivalent scattering particle radius decreases while the particle density increases. According to theory, the smaller the particle, the more obvious is the isotropic scattering, so that the anisotropy factor decreases in the case of thermally induced tissue coagulation. The significant difference of the absolute values may be due to the different models adopted. The literature assumed that all of the particles had the same size and adopted the single irrelevant scattering model ($\mu_s' = N_0 \pi r^2 Q_{\mathrm{scat}}(1-g)$). This paper assumes that the particle sizes are different and the particle content follows an exponential distribution, which is more in accordance with realistic biological tissue. The average equivalent scattering particle radius of normal rat brain tissue calculated by Mie theory is exactly in the range of biological tissue mitochondria radius. Several studies[19,21] have identified mitochondria as the primary scatterers in tissue. The main factor that affects scattering in biological tissue is the content of mitochondria.

5. Conclusions

(1) There is a close relationship between μ_s' and the degree of thermal coagulation of biological organization. The degree of thermally induced tissue coagulation can be obtained by the value of μ_s'. It is around 50°C for the critical temperature between reversible and irreversible changes of μ_s' of biological tissue.

(2) The average equivalent scattering particle radius calculated by Mie theory can be used as an evaluation parameter for optical properties of biological tissue. When biological tissue coagulates by heating, the reduced scattering coefficient μ_s' increases, the average equivalent scattering particles radius decreases, the particle density increases, and the anisotropy factor decreases.

Acknowledgment

This study was supported by the National Natural Science Foundation (Grant No. 30671997) and the National High Technology Research and Development Program of China (No. 2008AA02Z438).

References

1. S. Xie, H. Li, B. Li, "Measurement of optical penetration depth and refractive index of human tissue," *Chin. Opt. Lett.* **1**(1), 44–46 (2003).
2. D. Zhu, Q. Luo, S. Zeng, J. Yu, Y. Ruan, "Study on kinetics of thermally induced damage of rat liver with light scattering technique," *Chin. J. Lasers* **29**(7), 667–672 (2002).
3. G. Marquez, L. V. Wang, S. P. Lin, J. A. Schwartz, S. L. Thomsen, "Anisotropy in the absorption and scattering spectra of chicken breast tissue," *Appl. Opt.* **37**(4), 798–804 (1998).
4. B. Li, S. Xie, Z. Lu, "Spectral properties of new photosensitizers for photodynamic diagnosis and therapy," *Spectroscopy and Spectral Analysis* **22**(6), 902–904 (2002).
5. R. Chen, S. Xie, Y. Chen, A. Lin, D. Li, "Optical parameters of Chinese blood," *J. Optoelectronics Laser* **13**(1), 92–97 (2002).
6. L. V. Wang, S. L. Jacques, "Source of error in calculation of optical diffuse reflectance from turbid media using diffusion theory," *Comp. Meth. Prog. Biomed.* **61**(3), 163–170 (2000).

7. D. Zhu, Q. Luo, G. Zhu, W. Liu, "Kinetic thermal response and damage in laser coagulation of tissue," *Lasers Surg. Med.* **31**(5), 313–321 (2002).
8. W. C. Lin, C. Buttemere, A. Mahadevan-Jansen, "Effect of thermal damage on the *in vitro* optical and fluorescence characteristics of liver tissues," *IEEE J. Sel. Top. Quantum Electron.* **9**(2), 162–170 (2003).
9. H. J. Schwarzniaier, T. Goldbach, I. Yaroslavsky, *et al.*, "Optical changes of porcme brain tissue after thermal coagulation," *SPIE* **2391**, 451–457 (1995).
10. H. Wei, D. Xing, G. Wu, H. Gu, J. Lu, B. He, "Changes and thermal coagulation of human liver tissue induced changes in the optical properties of liver tissue at KTP/YAG laser *in vitro*," *Chin. J. Lasers* **33**(6), 852–856 (2006).
11. L. Dai, "Research on real time, *in vivo*, minimal invasive measurement of brain tissues' parameters by near infrared spectroscopy and its application," Nanjing University of Aeronautics and Astronautics, Nanjing (2008).
12. Y. Zhang, Q. Wang, H. Lu, J. Lai, Z. Li, "Equivalent particle's model of biological tissue and calculation of Mie phase function," *Acta Laser Biology Sinica* **16**(1), 79–83 (2007).
13. Q. Wang, Y. Zhang, J. Lai, Z. Li, A. He, "Application of Mie theory in biological tissue scattering characteristics analysis," *Acta Physica Sinica* **56**(2), 1023–1027 (2007).
14. X. Wang, B. W. Pogue, S. Jiang, X. Song, K. D. Paulsen, C. Kogel, S. P. Poplack, W. A. Wells, "Approximation of Mie scattering parameters in near-infrared tomography of normal breast tissue *in vivo*," *J. Biomed. Opt.* **10**(5), 051704 (2005).
15. X. Wang, B. W. Pogue, S. Jiang, H. Dehghani, X. Song, S. Srinivasan, B. A. Brooksby, K. D. Paulsen *et al.*, "Image reconstruction of effective Mie scattering parameters of breast tissue *in vivo* with near-infrared tomography," *J. Biomed. Opt.* **11**(4), 041106 (2006).
16. C. Matzler, "MATLAB functions for Mie scattering and absorption," IAP Research Report No. 2002-08 (2002).
17. M. Bartek, X. Wang, W. Wells, K. D. Paulsen, B. W. Pogue, "Estimation of subcellular particle size histograms with electron microscopy for prediction of optical scattering in breast tissue," *J. Biomed. Opt.* **11**(6), 064007 (2006).
18. Z. Qian, "Study of near infrared guidance technique for 3D targeted localization in neuro-surgery for Parkinson's disease," Nanjing University of Aeronautics and Astronautics, Nanjing (2003).
19. A. M. K. Nilsson, C. Sturesson, D. L. Liu, S. Andersson-Engels, "Changes in spectral shape of tissue optical properties in conjunction with laser-induced thermotherapy," *Appl. Opt.* **37**(7), 1256–1267 (1998).
20. J. Swartling, S. Pålsson, P. Platonov, S. B. Olsson, S. Andersson-Engels, "Changes in tissue optical properties due to radio-frequency ablation of myocardium," *Med. Biol. Eng. Comput.* **41**(4), 403–409 (2003).
21. B. Beauvoit, T. Kital, B. Chance, "Contribution of the mitochondrial compartment to the optical properties of the rat liver: A theoretical and practical approach," *Biophys. J.* **67**(6), 2501–2510 (1994).